

This copy is for your personal, non-commercial use only.

If you wish to distribute this article to others, you can order high-quality copies for your colleagues, clients, or customers by [clicking here](#).

Permission to republish or repurpose articles or portions of articles can be obtained by following the guidelines [here](#).

The following resources related to this article are available online at www.sciencemag.org (this information is current as of September 30, 2010):

Updated information and services, including high-resolution figures, can be found in the online version of this article at:

<http://www.sciencemag.org/cgi/content/full/328/5978/593>

Supporting Online Material can be found at:

<http://www.sciencemag.org/cgi/content/full/science.1181348/DC1>

This article **cites 29 articles**, 8 of which can be accessed for free:

<http://www.sciencemag.org/cgi/content/full/328/5978/593#otherarticles>

This article has been **cited by** 2 article(s) on the ISI Web of Science.

This article has been **cited by** 3 articles hosted by HighWire Press; see:

<http://www.sciencemag.org/cgi/content/full/328/5978/593#otherarticles>

This article appears in the following **subject collections**:

Cell Biology

http://www.sciencemag.org/cgi/collection/cell_biol

Systematic Analysis of Human Protein Complexes Identifies Chromosome Segregation Proteins

James R. A. Hutchins,^{1*} Yusuke Toyoda,^{2*} Björn Hegemann,^{1*†} Ina Poser,^{2*} Jean-Karim Hériché,^{3,4} Martina M. Sykora,¹ Martina Augsburg,² Otto Hudecz,¹ Bettina A. Buschhorn,¹ Jutta Bulkescher,⁴ Christian Conrad,⁴ David Comartin,^{5,6} Alexander Schleiffer,¹ Mihail Sarov,² Andrei Pozniakovsky,² Mikolaj Michal Slabicki,² Siegfried Schloissnig,^{2,7} Ines Steinmacher,¹ Marit Leuschner,² Andrea Ssykor,² Steffen Lawo,^{5,6} Laurence Pelletier,^{5,6} Holger Stark,⁸ Kim Nasmyth,^{1‡} Jan Ellenberg,⁴ Richard Durbin,³ Frank Buchholz,² Karl Mechtler,¹ Anthony A. Hyman,^{2,§} Jan-Michael Peters^{1§}

Chromosome segregation and cell division are essential, highly ordered processes that depend on numerous protein complexes. Results from recent RNA interference screens indicate that the identity and composition of these protein complexes is incompletely understood. Using gene tagging on bacterial artificial chromosomes, protein localization, and tandem-affinity purification–mass spectrometry, the MitoCheck consortium has analyzed about 100 human protein complexes, many of which had not or had only incompletely been characterized. This work has led to the discovery of previously unknown, evolutionarily conserved subunits of the anaphase-promoting complex and the γ -tubulin ring complex—large complexes that are essential for spindle assembly and chromosome segregation. The approaches we describe here are generally applicable to high-throughput follow-up analyses of phenotypic screens in mammalian cells.

Phenotypic screens using random mutagenesis, systematic gene deletion, or RNA interference (RNAi) are powerful techniques for cataloguing gene function. To interpret the resulting genotype-phenotype relationships, detailed molecular analyses are required, among which protein localization and identification of protein interactions are particularly informative. In yeast, the modification of most genes at their endogenous loci with tag-coding sequences has been valuable for systems-wide analyses of protein function (1–4). In mammalian cells, however, large-scale localization and interaction studies of proteins

expressed under control of their own regulatory sequences have so far lagged behind phenotypic analysis. The MitoCheck consortium (www.mitocheck.org) has therefore used recombineering techniques (5) to develop a fast and reliable procedure for the introduction of genes tagged in bacterial artificial chromosomes (BACs) into human tissue culture cells. This technique allows the stable expression of genes under their own promoters at near-physiological levels (6). We have combined this “BAC TransgeneOmics” technology with large-scale protein localization and interaction experiments to characterize about 100 mitotic protein complexes (Fig. 1A). By using this combined approach, we discovered previously unknown subunits of the γ -tubulin ring complex (γ -TuRC) and the anaphase-promoting complex (APC/C), complexes that are essential for spindle assembly and chromosome segregation, respectively (7, 8).

Generation of a library of HeLa cell pools stably expressing green fluorescent protein (GFP)-tagged BACs. We chose to characterize proteins required for mitosis because this process is essential for eukaryotic life, is of relevance for tumor biology, and is known to depend on numerous protein complexes. Many of these had been characterized before, providing prior knowledge that we could use to control our approaches and to draw hypotheses for unknown genes. RNAi screens performed in *C. elegans*, *Drosophila*, and mammalian cells as well as proteomic studies have furthermore identified numerous uncharacterized proteins required for

mitosis (9–17). In addition, the MitoCheck consortium carried out a genome-wide RNAi screen by means of time-lapse imaging of chromosome segregation in live cells that provided detailed phenotypic information for the majority of human proteins (16).

From these screens and the literature, we selected 696 proteins (table S1) for C-terminal tagging with a combined localization affinity-purification (LAP) tag (18), using high-throughput BAC recombineering in *Escherichia coli* (6). In most cases, we tagged mouse genes and expressed them in human cells because this allows functional testing of the tagged proteins through RNAi-mediated depletion of their endogenous counterparts (19). N-terminal tags were introduced if C-terminal tagging failed or in some cases to validate data obtained with the C-terminal tag. We were able to tag and stably express 591 (89%) of the selected proteins in HeLa cells (fig. S1). For each gene, we obtained at least one non-clonal pool of stably expressing cells, resulting in a library of 657 pools. Using antibodies to the GFP moiety of the LAP tag, we could detect the tagged proteins in 559 pools (85%), corresponding to 504 unique proteins (77%), by means of immunofluorescence microscopy (IFM) (table S1 and fig. S1C).

Localization of mitotic proteins. First, we analyzed all cell pools in which a GFP signal could be detected for the intracellular localization of tagged proteins in interphase, metaphase, and telophase, using fixed cells stained with antibodies to GFP and α -tubulin, and 4',6-diamidino-2-phenylindole (DAPI) to visualize DNA (Fig. 1B). In mitotic cells, we observed specific association with centrosomes, spindles, kinetochores, chromosomes, cleavage furrows, midbodies, or cortical structures for 180 proteins, of which 25 had not been characterized in mitosis and 54 not at all (fig. S1C). For 14 proteins, we confirmed our fixed-cell data by means of time-lapse imaging of living cells (Fig. 1C and fig. S2).

To identify proteins with potential roles in spindle assembly, we localized in more detail 102 proteins that showed mitotic centrosome or spindle association. Of these, 23 had not been characterized in mitosis and 9 not at all. Immunofluorescence images were classified into 87 staining patterns at five different mitotic stages, resulting in specific localization trajectories (Fig. 1B and fig. S3). The frequency distribution of different patterns was scored manually, and the 102 proteins were clustered into 10 groups according to these scores (Fig. 2). Localization analysis with this resolution allowed separation even of complexes with very similar localization, such as the kinetochore complex MIS12 and the mitotic checkpoint complex (MCC), into separate localization trajectories (see fig. S3). In all cases, subunits of known complexes were recovered in the same clusters [chromosomal passenger complex (CPC), centralspindlin, MIS12, Aurora

¹Research Institute of Molecular Pathology (IMP), Dr. Bohr-Gasse 7, A-1030 Vienna, Austria. ²Max Planck Institute (MPI) for Molecular Cell Biology and Genetics, Pflotenhauerstrasse 108, D-01307 Dresden, Germany. ³Wellcome Trust Sanger Institute, Wellcome Trust Genome Campus, Hinxton, Cambridge CB10 1HH, UK. ⁴Cell Biology and Biophysics Unit, European Molecular Biology Laboratory, Meyerhofstrasse 1, D-69117 Heidelberg, Germany. ⁵Samuel Lunenfeld Research Institute, Mount Sinai Hospital, 600 University Avenue, Toronto, Ontario M5G 1X5, Canada. ⁶Department of Molecular Genetics, University of Toronto, Toronto, Ontario M5S 1A8, Canada. ⁷German Cancer Research Center, Im Neuenheimer Feld 280, 69120 Heidelberg, Germany. ⁸Max Planck Institute for Biophysical Chemistry, Am Fassberg 11, D-37077 Göttingen, Germany.

*These authors contributed equally to this work.

†Present address: Institute of Biochemistry, Eidgenössische Technische Hochschule Zürich, Schafmattstrasse 18, CH-8093 Zürich, Switzerland.

‡Present address: Department of Biochemistry, University of Oxford, South Parks Road, Oxford OX1 3QU, UK.

§To whom correspondence should be addressed. E-mail: hyman@mpi-cbg.de (A.A.H.); peters@imp.univie.ac.at (J.-M.P.)

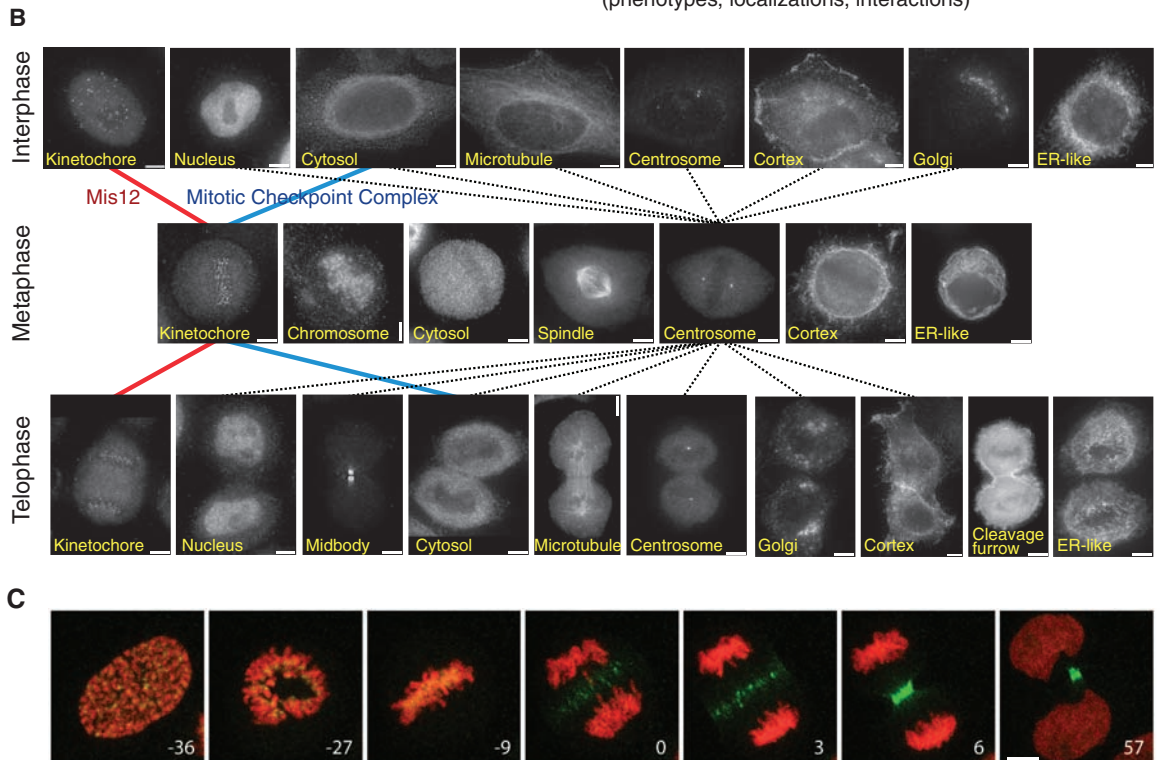
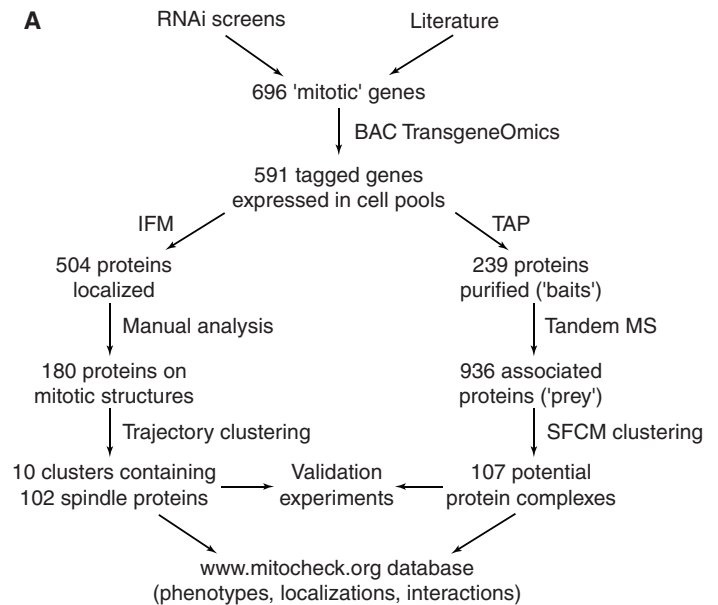
A-targeting protein for Xklp2 (TPX2), and γ -TuRC], although prior knowledge about the existence of these complexes had not been used to “train” the cluster algorithm. This suggests that clustering of localization trajectories can be used to formulate hypotheses about functions and physical interactions of uncharacterized proteins. For example, centrosomal protein of 120 kD (CEP120) clustered with proteins required for centriole duplication, suggesting that CEP120 may have a role in this process. RNAi experiments indicated that this is indeed the case (fig. S4).

Identification of mitotic protein complexes.

To characterize mitotic protein complexes, we isolated LAP-tagged proteins from cells arrested in mitosis using tandem-affinity purification (TAP) (fig. S5) (6). Samples were analyzed with SDS-polyacrylamide gel electrophoresis (SDS-PAGE) followed by silver staining and with in-solution trypsinization and tandem mass spectrometry (MS). Initially, proteins were selected on the basis of localization identified by means of GFP imaging or on reported mitotic functions. Once interaction partners had been identified, interaction mapping was performed iteratively

by producing new LAP-tagged cell pools to validate a subset of the interactions through reciprocal analyses. In total, cell pools containing 254 different tagged genes were analyzed. In 239 cases (94%), the “bait” proteins could be identified. These interacted with a total of 936 “prey” proteins that were present in specific samples, corresponding to 2011 distinct pair-wise interactions (20). Other proteins, which were found in more than 4.5% of all samples or in “mock” purifications, were excluded from further analyses because these proteins might represent contaminants (tables S2 and S3). For a complete pre-

Fig. 1. Use of BAC TransgeneOmics for identification and characterization of mitotic protein complexes in human cells. **(A)** Schematic outline of the workflow established for BAC tagging, GFP localization, and TAP-MS of mitotic proteins. **(B)** Representative images of fixed HeLa cells, obtained by means of IFM with antibodies to GFP. Examples are shown of cells that stably express LAP-tagged proteins that have different locations in interphase, metaphase, or telophase, as indicated in the images. Images are connected by lines that represent a subset of the localization trajectories observed for different proteins. The red and blue lines represent the trajectories of MIS12 and MCC, respectively. Dotted lines represent all observed trajectories that include centrosome localization in metaphase. Scale bar, 10 μ m. **(C)** Time-lapse images of a mitotic HeLa cell stably expressing H2B-mCherry (red) and the CPC subunit INCENP-LAP (green). Numbers indicate time (minutes) before and after anaphase onset. Scale bar, 10 μ m.



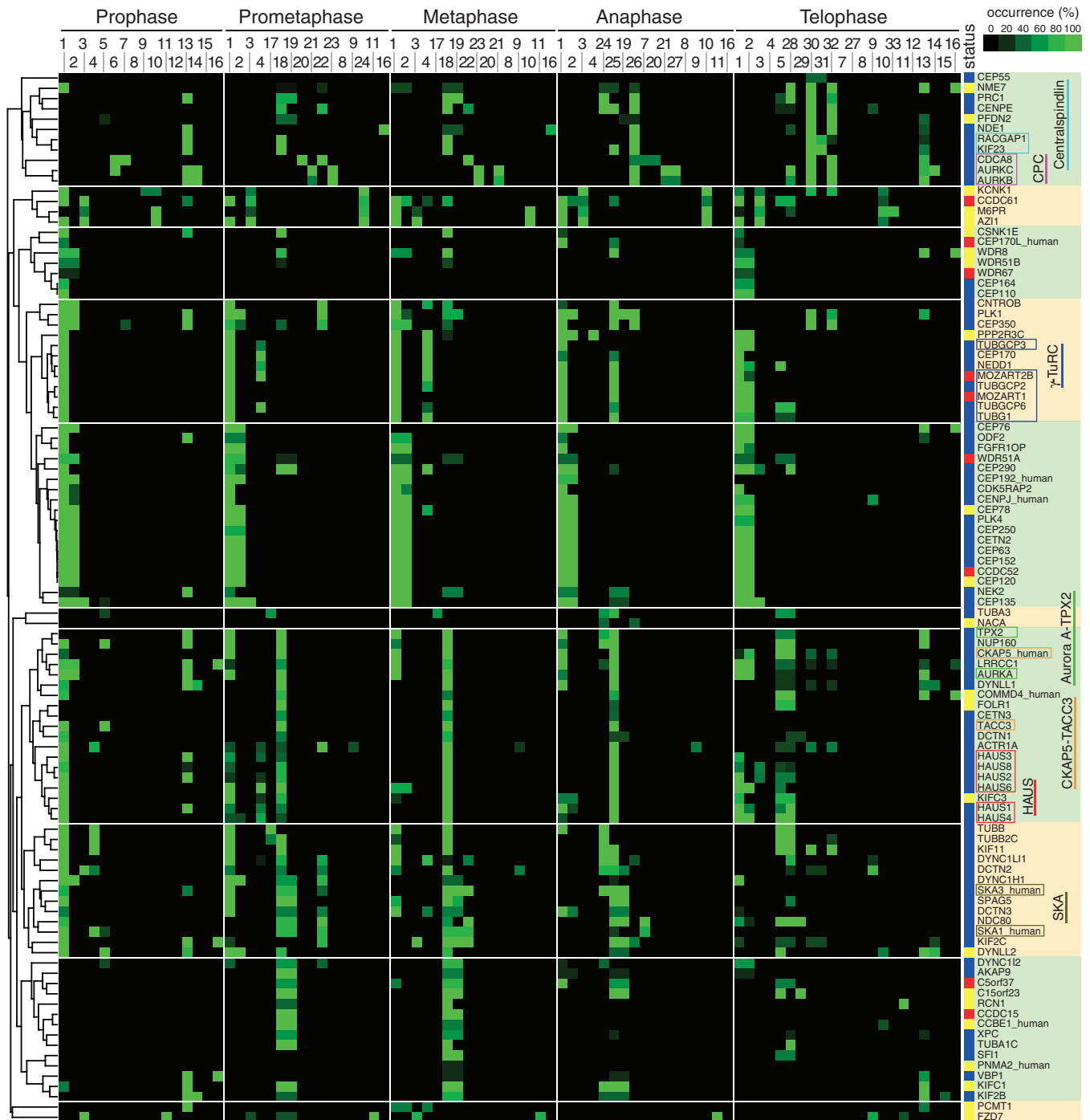


Fig. 2. Heat map showing hierarchical clustering of the localization trajectories of 102 spindle and centrosome proteins. IFM images of fixed HeLa cells expressing LAP-tagged proteins (listed on the y axis) in five mitotic phases were classified into 33 staining patterns (mouse ortholog proteins were imaged unless suffixed as “_human”). The frequency with which each staining pattern was observed for each protein in each phase is represented by a square, with color ranging from black (0% occurrence) to bright green (100% occurrence). The number codes for the staining patterns are as follows: 1, centrosome (PCM-like); 2, centrosome (fine dots); 3, dots near centrosome; 4, centrosome and partial microtubule (MT); 5, microtubule; 6, chromosome; 7, kinetochore; 8, cortex (whole); 9, cortex (partial); 10, dots in cytoplasm; 11, ER-like meshwork; 12, nuclear envelope; 13, nucleus; 14, dots in nucleus; 15, nucleolus; 16, whole cell; 17, spindle MT (whole); 18, spindle MT (K-fiber); 19, spindle matrix-like; 20, chromosome (axis); 21, chromosome (periphery); 22, kinetochore (sisters); 23, kinetochore (inner); 24, microtubule (whole); 25, microtubule (K-fiber);

26, spindle midzone; 27, cleavage furrow; 28, microtubule next to midbody; 29, microtubule (unclear); 30, midbody; 31, midbody ring; 32, midbody next to ring; and 33, Golgi-like. The “status” column shows the characterization status of each gene, as defined by literature searching in PubMed, according to the following color scheme: blue, reported to be involved in mitosis; yellow, some function reported but not in the context of mitosis; and red, functionally uncharacterized. The dendrogram on the left indicates the relative similarities of the trajectories of individual proteins to the entire trajectory pattern. The clustered heat map was divided into 10 subclusters on the basis of a visual inspection of clustered localization patterns (subclusters indicated by alternating green and yellow shading). The names of subunits of previously identified complexes are boxed in different colors (Centralspindlin, light blue; CPC, magenta; γ -TuRC, dark blue; Aurora A-TPX2, bright green; chTOG-TACC3, orange; Augmin/HAUS, red; SKA, olive-green).

presentation of all data, see www.mitocheck.org. Additional information on tagged BACs can be found at <http://hymanlab.mpi-cbg.de/BACE>.

We analyzed baits from 11 previously described reference complexes which, according to the literature, contain 74 subunits (fig. S6A). Our experiments identified 70 of these, indicating a low false-negative detection rate (fig. S6B). In 175 cases, our experiments revealed interactions between two proteins, both of which had been tagged and used as baits. Of these interactions, 94 (54%) could be detected with both baits. This frequency of reciprocal interactions is higher than in previous studies performed in yeast [15% in (3); 8% in (4)]. These results suggest that the number of false-positive interactions in our data set is relatively low. However, we cannot exclude that some false-positive interactions were detected.

To identify previously unknown complexes, we analyzed the data set of all interactions for the presence of proteins that are densely con-

nected with each other (fig. S7) using a clustering algorithm that we call spectral fuzzy C-means (SFCM). We identified 35 singletons (cases in which only the bait had been found), 107 clusters that contain between two and 20 proteins, and 13 clusters with more than 20 components (Fig. 3, figs. S7 and S8, and table S4). The 13 large clusters contain sets of loosely connected proteins, which presumably had been grouped together because the density of the interaction network was not high enough to separate these proteins into smaller, more meaningful clusters. However, among the 107 small clusters 11 matched the reference complexes with an average precision of 59% (the fraction of cluster members that belong to the same reference complex) and an average recall of 89% (the fraction of the reference complex subunits assigned to the same cluster). These values indicate that many of the small clusters represent bona fide protein complexes or groups of closely related complexes (for example, different isoforms of co-

hesin complexes clustered together) (table S4). As an example, Fig. 3 shows a graphical representation of 10 of the 107 small clusters and how they compare with reference complexes described in the literature. The entire interaction network can be seen in the supporting visualization S1 file.

Identification and characterization of mitotic protein complexes by combined interaction and localization studies. To test whether co-purifying proteins interact *in vivo*, we analyzed in how many cases similar localization patterns had been obtained for interacting proteins. We manually annotated a subset of 728 interactions and found that 49% of all pairwise interacting bait and prey proteins had similar localizations. This frequency was even higher (79%) when only reciprocally confirmed interactions were considered (fig. S9). For example, we observed that CEP120 both co-localized and physically interacted with coiled coil domain-containing 52 (CCDC52), suggesting that these proteins form a complex

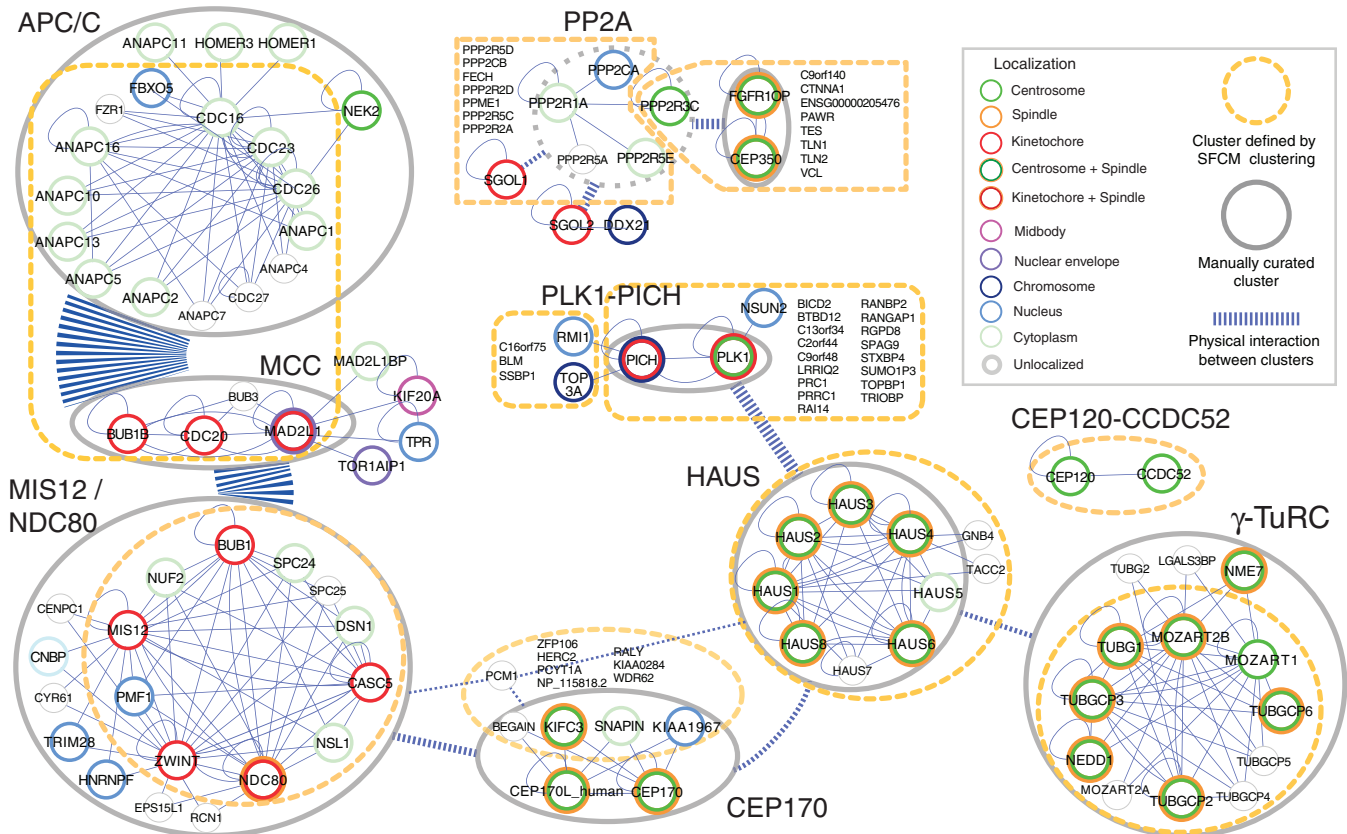


Fig. 3. Combined interaction and localization map for a selection of 10 out of 107 small clusters (cluster size, 2 to 20 proteins). Protein interaction data obtained by means of TAP-MS were analyzed with SFCM clustering. The resulting clusters (enclosed by orange dashed lines) were manually annotated according to literature knowledge (for composition of reference complexes as described in the literature, see fig. S6) (29). The resulting curated clusters are shown as gray ellipses: Complexes containing reciprocal interactions are enclosed by solid gray lines, whereas those without reciprocal interactions are denoted by dashed gray lines. Inter- and intra-cluster interactions are represented by dashed and solid blue lines, respectively, with the number of in-

teractions corresponding to the thickness of these lines. Localization as determined by use of GFP imaging is shown in the color codes as indicated. Cluster and protein complexes can have interactions with several other clusters/complexes. For example, MCC co-purified and therefore co-clustered both with APC/C and with the MIS12/NDC80 cluster. The former association reflects binding of MCC to APC/C in prometaphase cells (30), from which these proteins were purified, whereas MCC association with MIS12/NDC80 may reflect recruitment of MCC components to unattached kinetochores in prometaphase (31). For an expanded “master map,” integrating localization and interaction data for more proteins, see fig. S8.

(Figs. 2 and 3). Similarly, we observed that eight proteins, which had not been characterized when we performed our experiments, interacted reciprocally with each other and were all located on mitotic spindles (fig. S10). These proteins are subunits of the Augmin/HAUS complex, which has recently been shown to be essential for spindle function (21–23). Combining localization and interaction data can also identify unknown interactions between well-characterized proteins and complexes, as is illustrated by our finding that Polo-like kinase 1-interacting checkpoint helicase [PICH, also known as excision repair cross-complementing rodent repair deficiency, complementation group 6-like (ERCC6L)] interacts and co-localizes on chromosome bridges

with subunits of the RTR complex [RecQ helicase (BLM)-topoisomerase III (TOP3A)–RecQ mediated genome instability 1 (RMI1) complex] (fig. S11) (24).

Identification of C10orf104 as a subunit of the APC/C. We further characterized chromosome 10 open reading frame 104 (C10orf104) because this 11.7-kD protein co-purified with seven different APC/C subunits (fig. S12A), but not with any other bait, and thus co-clustered with the APC/C in our SFCM analysis (Fig. 3). The APC/C is a 1.5-MD ubiquitin ligase complex that is essential for chromosome segregation and mitotic exit (8). Because APC/C has been characterized in detail, it was surprising that a previously uncharacterized protein co-purified with

APC/C subunits. However, when C10orf104 also was used as bait several APC/C subunits were detected (fig. S12A), and antibodies raised against C10orf104 immunoprecipitated the entire APC/C and its associated cyclin B ubiquitylation activity (Fig. 4, A and B). Immunoblot experiments showed that C10orf104 is present throughout the cell cycle (fig. S12, B and C), and density gradient centrifugation experiments indicated that most of C10orf104 is associated with the APC/C (Fig. 4C). These observations indicate that C10orf104 is a constitutive subunit of the APC/C and not a substrate or a transiently associating regulatory protein. Electron microscopic analysis of APC/C labeled with antibodies to C10orf104 suggested that C10orf104 is located at the top of APC/C's "arc lamp" domain, in the vicinity of the subunit CDC27 (Fig. 4D and fig. S12, D to F). The amino acid sequence of C10orf104 is highly conserved among vertebrates (95% identical between human and zebrafish), suggesting that despite its small size, this protein performs an important function within the APC/C. Related sequences also exist in invertebrates (fig. S12G), although we could not yet identify homologous sequences in yeast. These observations indicate that C10orf104 is an evolutionarily conserved APC/C subunit, which we propose to call APC16 (gene symbol ANAPC16). We suspect that APC16 has previously escaped detection in protein gels or through MS because of its small size.

Identification of proteins interacting with the γ -TuRC. We also characterized chromosome 13 open reading frame 37 (C13orf37) and two closely related proteins, called family with sequence similarity 128 member A and member B (FAM128A and FAM128B), because these proteins co-purified with three different subunits of the γ -TuRC. This complex is located at centrosomes and mediates the formation of bipolar spindles in mitosis (7). When C13orf37 and FAM128B were used as baits, all six known γ -TuRC subunits were identified (Fig. 3 and Fig. 5, A and B). Sucrose density gradient centrifugation experiments confirmed that C13orf37 and FAM128B are associated with the γ -TuRC component tubulin gamma 1 (TUBG1) (fig. S13A). Similar to γ -TuRC subunits, C13orf37 and FAM128B were located on centrosomes throughout the cell cycle and to a lesser extent on mitotic spindles (Fig. 2, Fig. 5, C and D, and fig. S13B). Proteins homologous to C13orf37 and FAM128A/B are predicted to exist in many eukaryotes, including in the case of C13orf37 the fission yeast *Schizosaccharomyces pombe* (fig. S13, C and D). However, the corresponding genomic sequences have not been annotated as genes in all organisms, possibly because C13orf37 and FAM128A/B are small proteins of 8.5 and 16.2 kD, respectively. C13orf37 and FAM128A/B may thus be evolutionarily conserved γ -TuRC subunits that previously may not have been detected because of their small size. However, unlike the known subunits of γ -TuRC [tubulin, gamma complex–

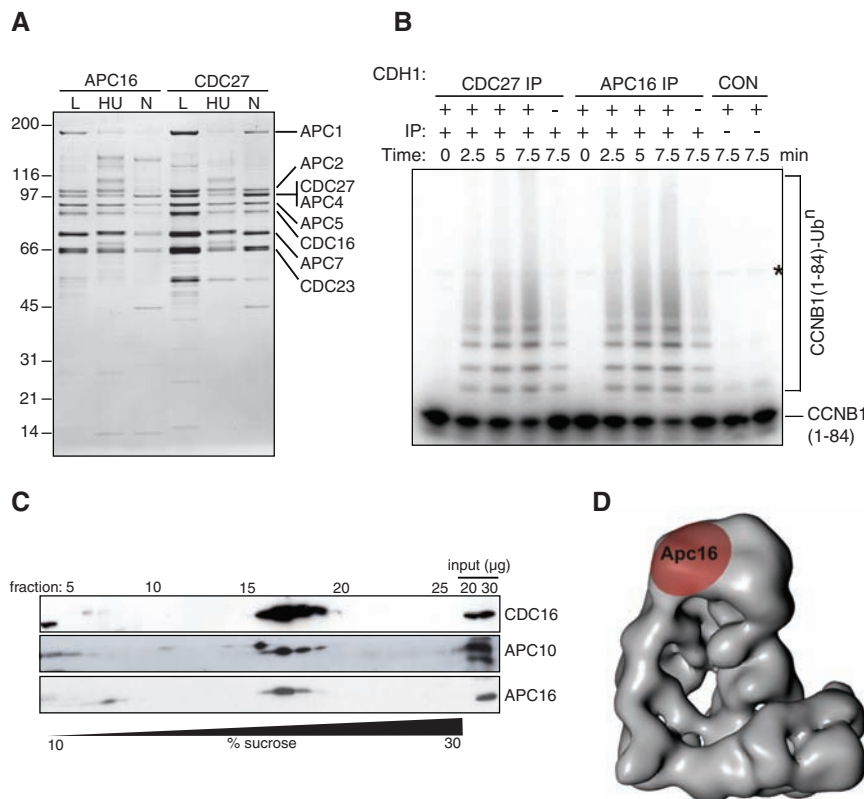
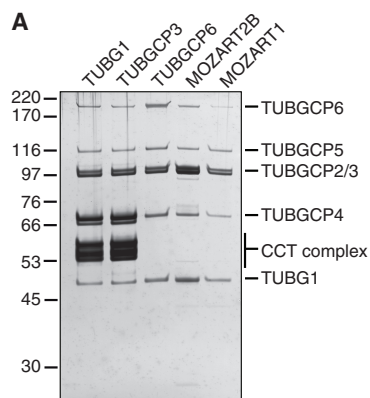


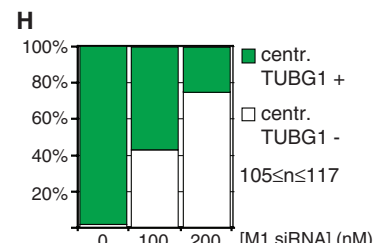
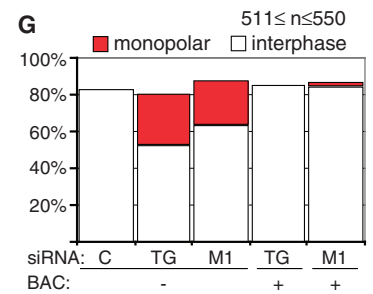
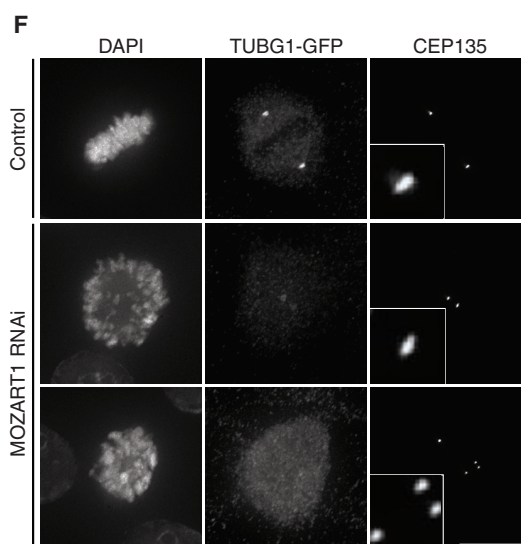
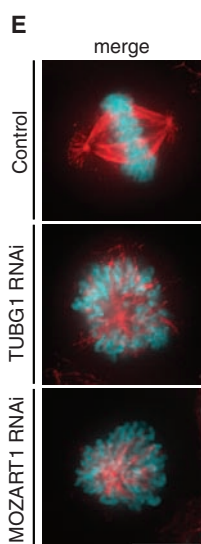
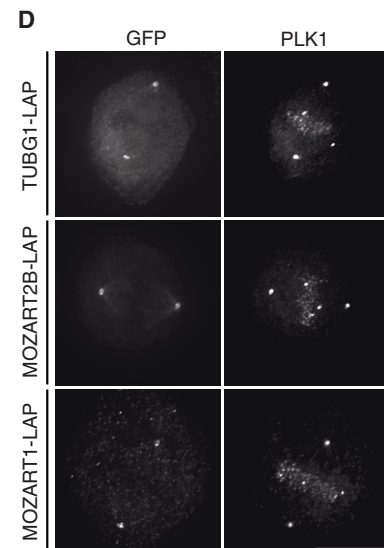
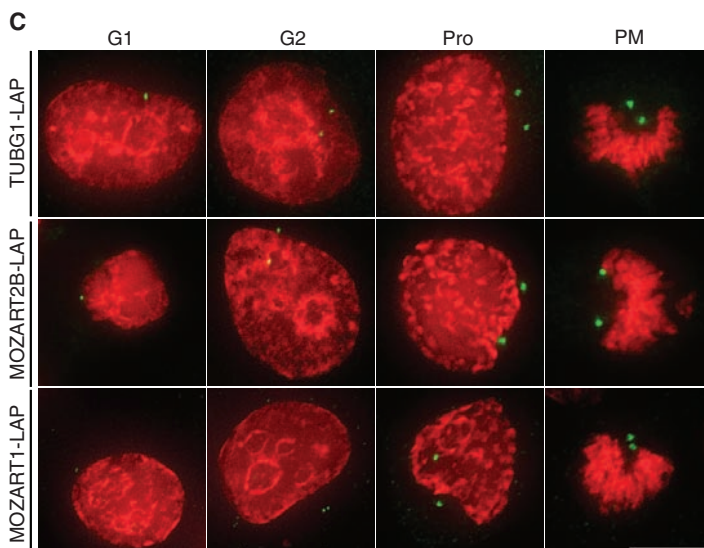
Fig. 4. Characterization of APC16, a previously unknown subunit of the APC/C. **(A)** Silver-stained SDS-PAGE gel showing proteins immunoprecipitated by using antibodies to APC16 or CDC27 from extracts of HeLa cells, cultured under logarithmic growth conditions (L), or arrested in S phase by means of treatment for 18 hours with hydroxyurea (HU) or arrested in prometaphase by treatment for 18 hours with nocodazole (N). Numbers on the left indicate the molecular masses of reference proteins. **(B)** Phosphorimage showing the ubiquitylation of Cyclin B1 (CCNB1), catalyzed by CDC27 and APC16 immunoprecipitates. [¹²⁵I]-labeled human CCNB1 fragment (amino acids 1 to 84) was incubated with CDC27 or APC16 immunoprecipitates from logarithmically growing HeLa cells, plus E1 and E2 enzymes, ubiquitin, and adenosine 5'-triphosphate (ATP), with or without the recombinant co-activator protein CDH1, for the times indicated and then analyzed with SDS-PAGE and phosphorimaging. CON indicates empty protein-A beads (left) and a condensin antibody immunoprecipitate (right). The asterisk marks a contaminating band present in the CCNB1 sample. **(C)** Immunoblots showing the co-sedimentation of APC16 with core APC/C subunits CDC16 and APC10, after density gradient centrifugation. An extract of logarithmically growing HeLa cells was subjected to centrifugation through a 10 to 30% sucrose density gradient. Twenty-eight fractions were collected and analyzed with SDS-PAGE and immunoblotting with the antibodies indicated. **(D)** Three-dimensional model of the human APC/C obtained with electron microscopy (30) showing the location of APC16, as determined by means of antibody labeling.

Fig. 5. Characterization of the γ -TuRC interacting proteins MOZART1 and MOZART2B. **(A)** Silver-stained SDS-PAGE gel of LAP-purified TUBG1, TUBGCP3, TUBGCP6, MOZART2B, and MOZART1. Numbers on the left indicate the molecular masses of reference proteins. Proteins annotated according to expected electrophoretic mobility are listed on the right. CCT, chaperonin-containing T-complex.



B

Protein	Other name	Mass (kDa)	LAP-tagged bait				
			TUBG1	TUBGCP3	TUBGCP6	MOZART1	MOZART2B
TUBG1	γ -Tubulin	51.2	33.7%	85.6%	10.9%	11.8%	18.0%
TUBGCP2	GCP-2	102.5	28.8%	56.9%	23.2%	26.8%	51.7%
TUBGCP3	GCP-3	103.6	25.8%	55.4%	20.7%	21.6%	34.1%
TUBGCP4	GCP-4	76.1	15.2%	31.1%	9.5%	12.3%	30.5%
TUBGCP5	GCP-5	118.3	17.5%	20.8%	15.2%	18.1%	30.9%
TUBGCP6	GCP-6	200.5	12.0%	7.0%	18.1%	7.6%	16.1%
MOZART1	C13orf37	8.5	32.9%	52.4%	32.9%	34.6%	32.9%
MOZART2A	FAM128A	16.2	10.1%*	-	10.1%*	24.1%	24.1%
MOZART2B	FAM128B	16.2	-	51.9%	-	-	22.0%



(B) MS results obtained from the samples in (A), showing identification of γ -TuRC subunits plus MOZART1, MOZART2A, and MOZART2B. Entries highlighted in orange are bait proteins, yellow indicates proteins whose interaction with the bait has previously been reported, and a white background indicates that the interaction was previously unknown. Asterisks indicate proteins identified by a single peptide. **(C)** IFM images showing centrosomal localization of TUBG1, MOZART2B, and MOZART1 through the cell cycle [G₁ phase, G₂ phase, prophase (Pro), or prometaphase (PM)]. HeLa cells expressing the indicated proteins were fixed and stained with antibodies to GFP (green) and with DAPI (red). **(D)** IFM images showing localization of TUBG1, MOZART2B, and MOZART1 to centrosomes and the mitotic spindle in fixed LAP cells stained with antibodies to GFP and PLK1. All images in this figure are maximum-intensity projections of DeltaVision stacks. Scale bar, 10 μ m. **(E)** IFM images of HeLa cells treated for 72 hours with 100 nM siRNA specific to either TUBG1 or MOZART1. Cells were fixed and stained with DAPI (blue) and TUBA1A antibodies (red). Scale bar, 10 μ m. **(F)** IFM images of TUBG1-LAP HeLa cells treated for 72 hours with 100 nM siRNA against TUBG1 so as to deplete the endogenous TUBG1 and, simultaneously, transfected either with luciferase siRNA (control siRNA) or MOZART1 siRNA. Cells were fixed and stained with DAPI, GFP antibodies (to visualize TUBG1-LAP), and CEP135 (to stain centrosomes). Two distinct phenotypes were observed: CEP135 foci in close proximity to each other that colocalize with faint TUBG1-GFP foci (middle row) and CEP135 foci dispersed randomly throughout the cell with no detectable TUBG1-

GFP foci (bottom row). Insets in the third column are magnified fivefold to show one centrosome. Scale bar, 10 μ m. **(G)** Histogram showing quantification of the experiment described in (E). In addition, cells containing the mouse TUBG1-LAP or the mouse MOZART1-LAP (BAC +) were treated with 100 nM siRNA specific for TUBG1 or MOZART1, respectively, and fixed and stained as in (E). C, control; TG, TUBG1 siRNA; M1, MOZART1 siRNA. **(H)** Histogram showing quantification of the experiment described in (F). The number of cells with GFP-positive (TUBG1 +) or -negative (TUBG1 -) centrosomes was counted. The GFP-negative cells are a combination of both MOZART1-depletion phenotypes shown in (F).

associated proteins (TUBGCP2 to -6), C13orf37 and FAM128A/B do not contain the conserved “Spc97_Spc98” GCP domain (25). The TUBGCP nomenclature can therefore not be applied to C13orf37, FAM128A, or FAM128B. Instead, we propose to call these proteins mitotic-spindle organizing proteins associated with a ring of γ -tubulin (MOZART1, MOZART2A and MOZART2B, respectively).

MOZART1, an evolutionarily conserved protein essential for γ -TuRC function. To test whether the MOZARTs are important for γ -TuRC function, we performed RNAi experiments in HeLa cells. Transfection of MOZART2A/B small interfering RNA (siRNA) did not result in detectable mitotic phenotypes, but we cannot exclude that this was due to incomplete depletion of these proteins. In contrast, depletion of either MOZART1 or TUBG1 led to the accumulation of prometaphase cells with monopolar spindles and closely spaced centrosome pairs (Fig. 5, E to G). These phenotypes were fully reverted through stable integration of the corresponding LAP-tagged mouse genes on BACs (Fig. 5G), ruling out off-target RNAi effects and showing that the LAP-tagged proteins used for localization and interaction mapping are functional.

Monopolar spindle phenotypes have been observed after depletion of γ -TuRC, but also after inactivation of PLK1 (26) or Aurora A kinase (27). We therefore tested whether MOZART1 depletion could interfere with spindle assembly directly by preventing γ -tubulin recruitment to centrosomes, or indirectly by decreasing PLK1 or Aurora A activity. In IFM experiments, MOZART1-depleted cells were stained equally well as control cells with antibodies specific for phospho-epitopes generated by PLK1 or Aurora A (fig S13, E and F), suggesting that MOZART1 is not required for the activation of these kinases. However, depletion of MOZART1 did strongly reduce TUBG1-LAP-staining at centrosomes in 70% of the cells (Fig. 5, F and H). These observations indicate that MOZART1 is required for γ -TuRC recruitment to centrosomes. Because orthologs of MOZART1 exist in lower eukaryotes, including fission yeast, it is possible that this function has been highly conserved during evolution.

A human functional-genomics database. The data obtained in this study have enabled us to identify previously unknown protein complexes (CEP120-CCDC52 and Augmin/HAUS), new subunits of well-studied protein complexes such as the APC/C (APC16) and γ -TuRC (the MOZARTs), and unknown interactions between known proteins and complexes (PICH-RTR). However, the majority of our data has not yet been used for follow-up experiments. We suspect that such experiments will lead to additional important discoveries about the functions of human protein complexes in mitosis (28). This notion is supported by the observation that most of the protein

interactions detected in our experiments have not been previously reported. For example, for 60 of the 107 small SFCM clusters none of the interactions have been reported in seven major public-interaction databases (fig. S7A). Many of these clusters may therefore represent uncharacterized protein complexes. To enable the exploitation of these data by the scientific community, we have generated a human genome-wide database (www.mitocheck.org) that contains all data generated by the MitoCheck consortium (fig. S14). These include information on tagged BACs, immunofluorescence images obtained through GFP localization, silver-stained SDS-PAGE gels of all protein samples obtained through TAP, and all protein interaction lists obtained through in-solution trypsinization-tandem MS. In addition, this database contains movies from the MitoCheck RNAi screen, in which mitosis has been analyzed by means of live imaging of cells in which all human proteins have been targeted by siRNAs (16). The database also provides information about gene synonyms used in the literature, orthologs in other species, and protein interactions reported in public databases. This collection of localization, interaction, and phenotypic data will be a useful resource for understanding the functions of human proteins.

Conclusion. The widespread application of RNAi for phenotypic screens has not been accompanied by the development of approaches to rapidly study protein function. This means that it is difficult to characterize the results of such screens. Similar problems apply to the results of human genetic and genomic studies, which often identify many uncharacterized proteins potentially associated with disease. The combined use of BAC tagging, protein localization, and interaction mapping techniques that we describe here for mitotic proteins helps to overcome this limitation by allowing systems-scale approaches to studying protein function. These systematic nongenetic approaches represent a valuable counterpart to RNAi screens, in which limited penetrance and off-target effects can result in ambiguity in the identification of gene function. Rather than relying on phenotypic screens, hypotheses can be generated and tested from analysis of the protein complexes and localization of uncharacterized proteins.

References and Notes

1. S. Ghaemmaghami *et al.*, *Nature* **425**, 737 (2003).
2. W. K. Huh *et al.*, *Nature* **425**, 686 (2003).
3. A. C. Gavin *et al.*, *Nature* **440**, 631 (2006).
4. N. J. Krogan *et al.*, *Nature* **440**, 637 (2006).
5. Y. Zhang, F. Buchholz, J. P. Mueyrers, A. F. Stewart, *Nat. Genet.* **20**, 123 (1998).
6. I. Poser *et al.*, *Nat. Methods* **5**, 409 (2008).
7. U. Patel, T. Stearns, *Curr. Biol.* **12**, R408 (2002).
8. J. M. Peters, *Nat. Rev. Mol. Cell Biol.* **7**, 644 (2006).
9. P. Gönczy *et al.*, *Nature* **408**, 331 (2000).
10. J. S. Andersen *et al.*, *Nature* **426**, 570 (2003).

11. R. S. Kamath *et al.*, *Nature* **421**, 231 (2003).
12. B. Sönnichsen *et al.*, *Nature* **434**, 462 (2005).
13. G. Goshima *et al.*, *Science* **316**, 417 (2007).
14. R. Kittler *et al.*, *Nat. Cell Biol.* **9**, 1401 (2007).
15. M. P. Somma *et al.*, *PLoS Genet.* **4**, e1000126 (2008).
16. B. Neumann *et al.*, *Nature* **464**, 721 (2010).
17. M. Theis *et al.*, *EMBO J.* **28**, 1453 (2009).
18. I. M. Cheeseman, A. Desai, *Sci. STKE* **2005**, pl1 (2005).
19. R. Kittler *et al.*, *Proc. Natl. Acad. Sci. U.S.A.* **102**, 2396 (2005).
20. The protein interactions from this publication have been submitted to the International Molecular Exchange (IMEx) Consortium (<http://imex.sf.net>) through IntAct (www.ebi.ac.uk/intact), and assigned the identifier IM-11719.
21. G. Goshima, M. Mayer, N. Zhang, N. Stuurman, R. D. Vale, *J. Cell Biol.* **181**, 421 (2008).
22. S. Lawo *et al.*, *Curr. Biol.* **19**, 816 (2009).
23. R. Uehara *et al.*, *Proc. Natl. Acad. Sci. U.S.A.* **106**, 6998 (2009).
24. H. W. Mankouri, I. D. Hickson, *Trends Biochem. Sci.* **32**, 538 (2007).
25. R. D. Finn *et al.*, *Nucleic Acids Res.* **38** (Database issue), D211 (2010).
26. P. Lénárt *et al.*, *Curr. Biol.* **17**, 304 (2007).
27. E. Hannak, M. Kirkham, A. A. Hyman, K. Oegema, *J. Cell Biol.* **155**, 1109 (2001).
28. R. Kittler, L. Pelletier, F. Buchholz, *Cell Cycle* **7**, 2123 (2008).
29. Materials and methods are available as supporting material on Science Online.
30. F. Herzog *et al.*, *Science* **323**, 1477 (2009).
31. A. Musacchio, E. D. Salmon, *Nat. Rev. Mol. Cell Biol.* **8**, 379 (2007).
32. We are grateful to the following colleagues for their excellent assistance: E. Kreidl, M. Mazanek, M. Madalinski, G. Mitulović, M. Novatchkova, C. Stingl, Y. Sun (IMP and Institute of Molecular Biotechnology of the Austrian Academy of Sciences, Vienna); A. Bird, K. Kozak, D. Krastev, Z. Maliga, D. Richter, M. Theis, M. Toyoda (MPI, Dresden); P. Dube (MPI, Göttingen); and N. Kraut (Boehringer Ingelheim, Vienna). This work was funded in the most part by the European Commission via the Sixth Framework Programme Integrated Project MitoCheck (LSHG-CT-2004-503464). Work in the laboratories of J.-M.P. and K.M. received support from Boehringer Ingelheim, the Vienna Spots of Excellence Programme, the Austrian Science Fund Special Research Programme “Chromosome Dynamics,” and the Genome Research in Austria Programme. Work in the laboratories of A.A.H. and F.B. received support from the Max Planck Society and from Bundesministerium für Bildung und Forschung grants NGFN-2 SMP-RNAi (01GR0402) and NGFN-Plus (01GS0859). Work in the laboratory of L.P. was supported by operating grants from the Natural Science and Engineering Research Council of Canada (RGPIN-355644-2008), the National Cancer Institute of Canada (019562), and the Human Frontier Science Program (CDA0044/200). L.P. holds a Canada Research Chair in Centrosome Biogenesis and Function. Y.T. was supported by a Postdoctoral Fellowship for Research Abroad from the Japan Society for the Promotion of Science.

Supporting Online Material

www.sciencemag.org/cgi/content/full/science.1181348/DC1
Materials and Methods

Figs. S1 to S14

Tables S1 to S4

References

Supporting Visualization S1

31 August 2009; accepted 22 March 2010

Published online 1 April 2010;

10.1126/science.1181348

Include this information when citing this paper.